A Study on Real-time Control of Bead Height and Joint Tracking Using Laser Vision Sensor

H. K. Kim and H. Park

Abstract

There have been continuous efforts on automating welding processes. This automation process could be said to fall into two categories, weld seam tracking and weld quality evaluation. Recently, the attempts to achieve these two functions simultaneously are on the increase. For the study presented in this paper, a vision sensor is made, a vision system is constructed and using this, the 3 dimensional geometry of the bead is measured on-line. For the application as in welding, which is the characteristic of nonlinear process, a fuzzy controller is designed. And with this, an adaptive control system is proposed which acquires the bead height and the coordinates of the point on the bead along the horizontal fillet joint, performs seam tracking with those data, and also at the same time, controls the bead geometry to a uniform shape. A communication system, which enables the communication with the industrial robot, is designed to control the bead geometry and to track the weld seam. Experiments are made with varied offset angles from the pre-taught weld path, and they showed the adaptive system works favorable results.

Key Words : Laser vision sensor, Arc welding, Fuzzy control, Seam tracking, Bead height control.

1. Introduction

In welding automation system, the offset of the weld torch, bead width, weld pool size, and weld penetration are considered as significant factors deciding the geometry of weld product. Among these, the bead width and the weld penetration have close relationship with the weld quality.

For the study introduced in this paper, a multi-purpose vision system has been designed and constructed using diode laser and a CCD camera, which can be used for either seam tracking or monitoring. And the application of the system to the real-time measurement shows it provides 3 dimensional information in fair confidence. Many precedent studies give prior importance to bead width or weld pool width in the process of weld quality estimation.[1~3] In this study however, the bead height is measured in real-time, and with the data acquired, the bead geometry control and the seam tracking are performed simultaneously and effectively against those given disturbances of gravitational force and the offset angles of 3°, 4°, or 5° from the pre-taught weld path. An image processing algorithm dealing only with ROI(region of interest) is designed to the flexibility and faster performance of the program. A fuzzy controller is designed considering the heat-related welding processes, which are nonlinear and hardly defined. Errors and their derivatives of the sensor coordinates, x_S and z_S were taken as control input while weld torch shifts along the robot coordinate axes, x_R and z_R as control output.

H. K. Kim : Samsung SDI, Seoul, Korea
H. Park : Manufacturing Engineering R&D Team, KIA Motors, Kyungki, Korea
E-mail : hpark21@kia.co.kr

2. Vision sensor and system configuration

2.1 Vision sensor

The method of using constructed light (or light pattern) is adopted, and commercialized CCD camera and diode laser are used. A laser slit is constructed by passing through the cylindrical lens the collimated beam from the diode.

In designing vision sensor, base-line (distance between the laser source and the camera), the angle between the laser slit and the principal axis of the camera, the depth of view, and the field of view are important parameters which must be taken into consideration. The base-line, for instance, has a direct relationship with the size of the vision sensor.[6] For this reason and the capability to change the base line without changing the position of the laser source, two scanning mirrors were used. And, this results in the movement of the laser slit within the adjustable focal lengths of the camera. Though prism mirrors are used in general to make sure of the precision of the vision sensor, 1mm-thick normal mirrors are used as scanning mirrors. But, due to diffraction, the laser stripe resulted from the projection shows to be, instead of a clear thin stripe, a thick combination of rather bright center and edges less bright but could be noises. This hardware-related problem is resolved through the image-processing algorithm.

To minimize the weight of the vision sensor, 0.5 mm-thick steel plate was used for housing the camera, but the cooling system is not considered. The protecting mirrors in front of the laser and the camera are changeable. To separate the laser stripe from the arc and spatter noise, an optical filter and the protector are used. The protector is made with 0.7mm-thick plate to be able to endure the strong heat from the weld pool and the bead. The schematic diagram of the constructed vision sensor is as shown in Fig. 1, and the vision sensor mounted to the weld torch of an industrial robot in Fig. 2.

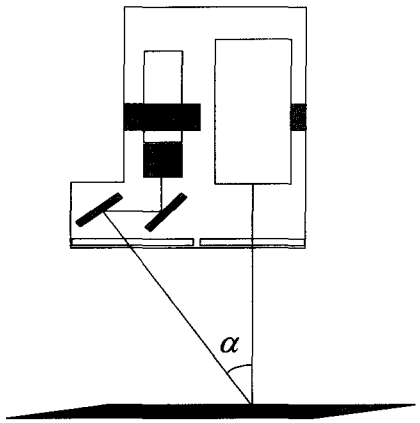

Fig. 1 Schematic diagram of vision sensor

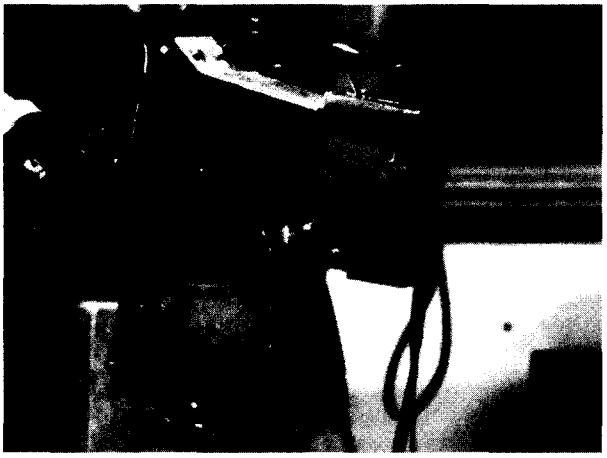

Fig. 2 Vision sensor mounted to the welding robot

2.2 System configuration

The configured system is shown in Fig. 3. A vision board with DSP(TMS320C31) installed is used as image grabber and processor. The power and the wavelength of the diode laser are 4.25mW and 670nm, respectively. And a band pass filter with center wavelength of 670nm and FWHM(full width half mean) of ±5nm is also used. When welding is in process in the direction shown in Fig. 3 the vision sensor 30mm offset to the rear of the weld torch captures the image of the bead and the weld joint and send it to the vision board. The vision board does the image processing needed to acquire feature data, and the fuzzy controller takes these data as input. The output of the controller is then transferred through

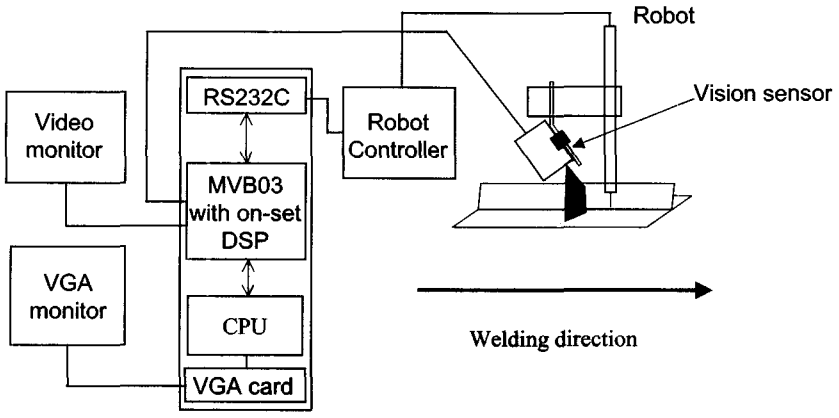

Fig. 3 System configurationl

RS232C to the robot controller.

3. Sensor calibration

3.1 Equations

Sensor calibration might be said to fall into 2 steps ; first to calculate the camera matrix and second, to define the light plane. Equation (1) and (2) can be acquired by applying homogeneous coordinate system to the image coordinates U, V.

$$U = u/h \tag{1}$$

$$V = v/h \tag{2}$$

When, between the point in space, P and its image coordinates P', are found the relationship as in equation (3), (4).

$$[x\ y\ z\ 1]\ T = [u\ v\ h] \tag{3}$$

$$T = \begin{bmatrix} C_{11} & C_{12} & C_{13} \\ C_{21} & C_{22} & C_{23} \\ C_{31} & C_{32} & C_{33} \\ C_{41} & C_{42} & C_{43} \end{bmatrix} \tag{4}$$

And, the laser plane is defined as in equation (5).

$$[\ x\ \ y\ \ z] \begin{bmatrix} a_1 \\ a_2 \\ a_3 \\ a_4 \end{bmatrix} = 0 \tag{5}$$

When **R** is defined as the matrix that is obtained by inserting image coordinates into the equation (1) ~ (5), and **W** as the one consisting of spatial coordinates, the sensor matrix, **M** can be gained as follows by Seudo-Inverse method.[4)]

$$\mathbf{M} = (\mathbf{R}^T\mathbf{R})^{-1}\mathbf{R}^T\mathbf{W} \tag{6}$$

3.2 Calibration experiment

A calibration block used in the calibration experiment has 5 steps of 2, 4, 6, 8, and 10mm height, all steps being a square of 19.1mm. Fig. 4 shows the calibration block with the laser stripe projected on.

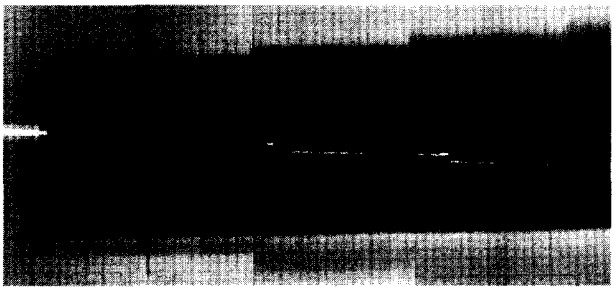

Fig. 4 Calibration block used in the experiment

15 data sets are used in the experiment, i.e., the real coordinates x, y, and z, and image coordinates U and V. The laser power is set to the best resolution achievable and varied points in each image frame are taken. Due to the limited capability of the system, the thickness of the laser stripe is about 0.4mm. Thus,

during the calibration experiment, all the gray values along the laser stripe in the image frame captured are examined and the pixel position having maximum gray level is considered to correspond with the spatial point in real coordinate system. Using a number of real points pre-recorded, the sensor matrix, M can be easily found. Repeated experiments confirmed that the sensor matrix can be trusted within the error of 0.06mm.

4. Image processing

4.1 Laser stripe extraction and thinning

In general, separating laser stripe from the captured iamge is called laser stripe extraction and finding the center line from the laser stripe, thinning. In the image processing algorithm used in this study, erosion filtering and LUT (look-up table) are applied to the raw image, and from the first column in the ROI (region of interest), the window, which is defined as certain number of pixels (here, 7) along the V axis, is applied consecutively down the V direction. Then, the window that has the most sum of gray values is taken, and the brightest pixel in that window is selected to be the pixel point for the start of the laser stripe. In the following column along the U axis, a window that has its center pixel at the position of the laser stripe pixel previously found is applied, the brightest pixel is selected. The process repeated in this way finds the laser stripe in an image frame and at the same time performs thinning. This algorithm, firstly, by adopting ROI oriented image processing, reduces the time needed for erosion filtering and LUT application from 820 msec to 122 msec, 85% decrease, and secondly, it can save additional time for the reason that it doesn't require the step setting a new threshold value for each image frame as in former method.[7] Fig. 5 shows the schematics of this algorithm.

4.2 Feature extraction

Feature data is explained to be feature points or feature lines that could give meanings to the algorithm applied. In this study, the point on the bead surface which has the maximum distance from the joint(i. e. height) and the joint point of the fillet are defined as feature data. In Fig. 6 marks the joint point, the point that has the same x_S coordinate as of the joint point, and the one farthest from the joint point, which are calculated real-time.

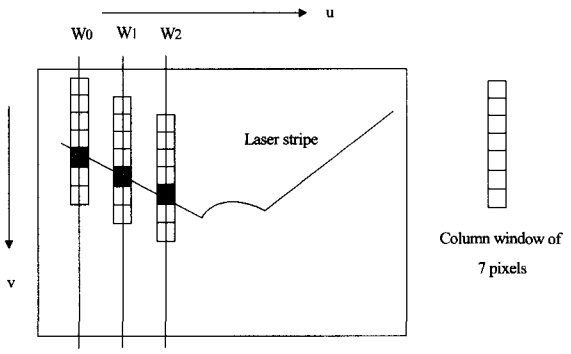

Fig. 5 Schematic diagram of laser stripe finding and thinning algorithm

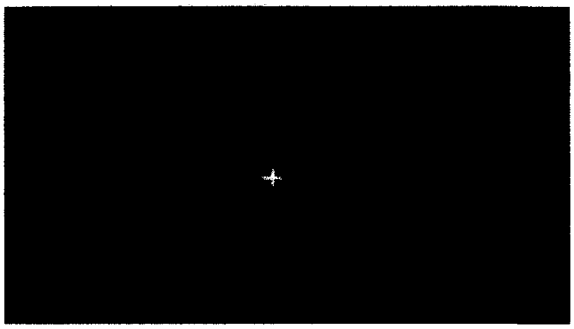

Fig. 6 Processed image and the found feature points

5. Experiment

5.1 Fuzzy controller

A fuzzy controller is designed to control the bead height or the distance of the point on the part of the bead surface, which falls in a certain range of angle and is farthest from the joint origin. Keeping the same bead height from the joint, it simultaneously tracks the weld seam.

FLC (fuzzy logic controller)[5] has been reported to work better results than conventional controllers where the system considered is too complicated and extremely nonlinear. A fuzzy controller, as shown in Fig. 7, consists of fuzzification interface, knowledge base, fuzzy inference, and defuzzification interface.

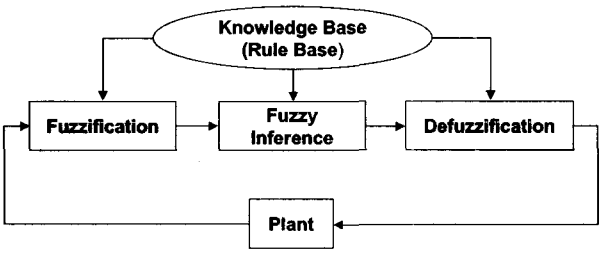

Fig. 7 Schematic diagram of fuzzy logic controller

Table 1 Fuzzy control rule

e \ △e	NB	NM	NS	ZO	PS	PM	PB
NB	PB	PB	PB	PM	PS	PS	ZO
NM	PB	PB	PM	PS	PS	ZO	NS
NS	PB	PM	PS	PS	ZO	NS	NS
ZO	PS	PS	PS	ZO	NS	NS	NM
PS	PS	PS	ZO	NS	NS	NM	NB
PM	PS	ZO	NS	NS	NM	NB	NB
PB	ZO	NS	NS	NM	NB	NB	NB

e : Respective errors for x_S and z_S
△e : Respective derivatives
NB : Negative Big PB : Positive Big
NM : Negative Medium PM : Positive Medium
NS : Negative Small PS : Positive Small
ZE : Zero

5.1.1 Fuzzy controller design

The designed FLC adopts the fuzzy singleton method to fuzzify the crisp data (measurement data) obtained by the vision sensor. These data and the control rules are defined in the rule base. And, those control rules together with Mamdani's inference are used to transform the fuzzy output to crisp data, which correspond to real control quantities. As for the defuzzification, simplified center of gravity method or weighted average method is used, which covers the weakness of the maximum height method and puts a stress to the fortes of the center of gravity method.

Fuzzy control rules are shown in Table 1. Fuzzy variables e, △e, and △u are defined as in Fig. 8, where those variables (e, △e, and △u) signifies the error, its derivative along the x_S and z_S axes and the output(torch shift) along the x_R and z_R axes. The actual variables corresponding to x_S and z_S coordinates are defined respectively.

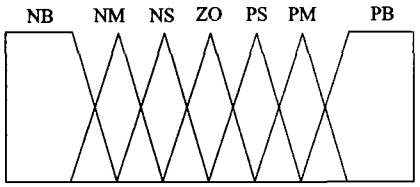

(a) Fuzzy variable for e

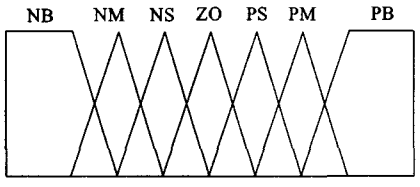

(b) Fuzzy variable for △e

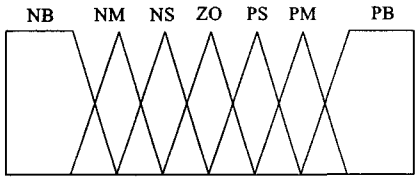

(c) Fuzzy variable for △u

Fig. 8 Fuzzy variables used in the experiment

5.2 Experiment set-up and method

5.2.1 Experiment set-up

In GMA (gas metal arc) welding of the horizontal fillet, the constructed vision sensor, industrial 6-axis robot (Nachi, model 7603AR), and arc welder are used. The shielding gas is 100% argon and the filler wire is of Ø 1.2mm. The weld current and voltage are set to 240A and 26V, respectively. CTWD (contact tip

to work-piece distance) is 15mm. The weld speed is 6 mm/s and the flow rate of the shielding gas is 15l/min. The coordinate system used is as shown in Fig. 9.

Due to the strong arc, it is extremely difficult to separate the laser stripe using only band pass filter. This necessitates the protector. The protector (Fig. 2) is made of 0.7mm-thick steel plate that can endure the strong heat transferred from the bead. It has a folding part that moves up and down along the bead in contact. This greatly minimizes the influence of the arc on captured images.

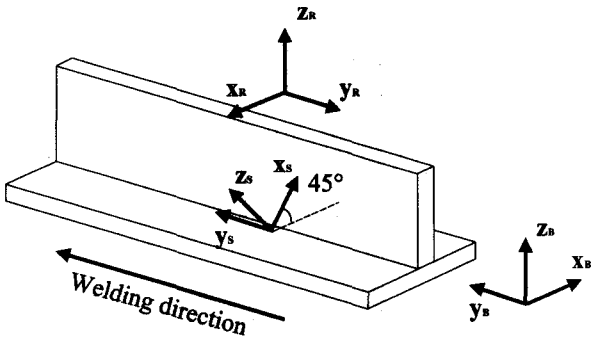

Fig. 9 Coordinate systems used in the experiment

5.2.2 Experiment method

The vision sensor that is fixed 30mm behind the weld torch measures the bead geometry and sends them as input to the fuzzy controller. The fuzzy controller responds by transferring the calculated output through RS232C to the robot controller. The output from the fuzzy controller are shift quantities along x_R and z_R axes.

By adjusting those two scanning mirrors prior to the experiment, the scan angle and the focal length of the camera are optimized. The laser slit is set to be vertical to the fillet while the camera is given a slant of about 15 degrees. With the given conditions, welding is performed repeatedly to find the representative geometry of the bead, which to be used to define fuzzy variables and reference inputs empirically.

The offset angle of 3°, 4°, or 5° between the pre-taught weld path and the real weld path and the gravitational force, which is common and makes the bead fall off the seam in horizontal fillet welding are considered as disturbances against the bead height control and the seam tracking. Fig. 10 describes this experiment method, and the algorithm used for the experiment is shown in Fig. 11.

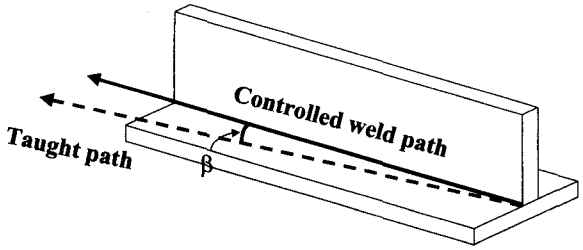

Fig. 10 Schematics of the experimental method

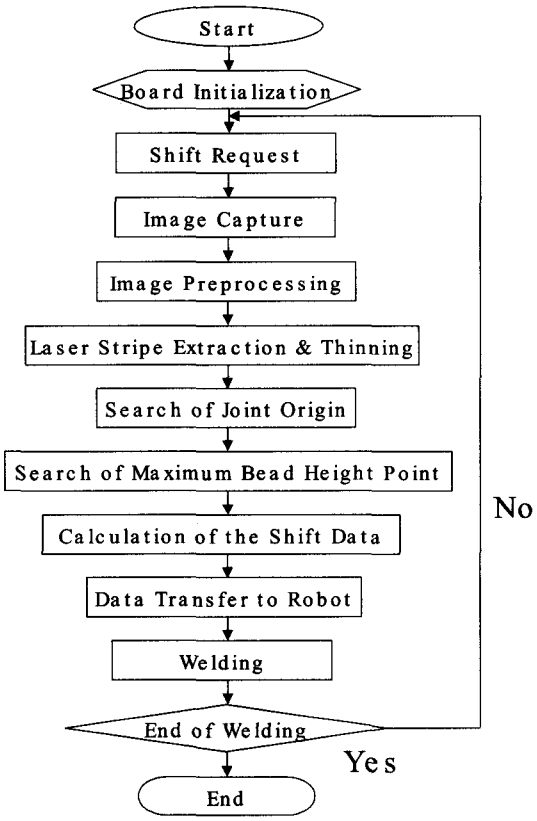

Fig. 11 Flow chart of the control

6. Results and discussion

Despite the arc and spatter noise, the bead was extracted effectively. With the help of the devised protector, real-time bead control and seam tracking

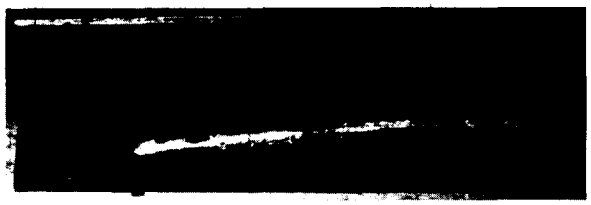

Fig. 12 Uncontrolled experiment result of 5 degrees deviation in horizontal fillet welding

Fig. 13 Controlled experiment result against 5 degrees deviation in horizontal fillet welding

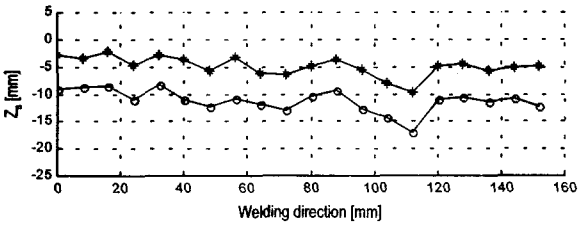

Fig. 14 Controlled z coordinate values against 5 degrees deviation

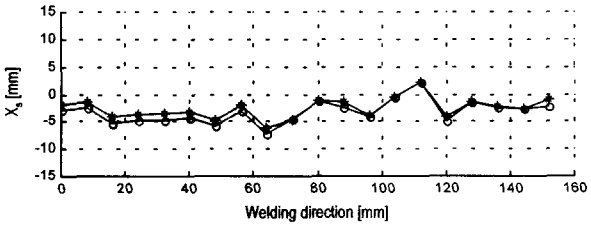

Fig. 15 Controlled x coordinate values against 5 degrees deviation

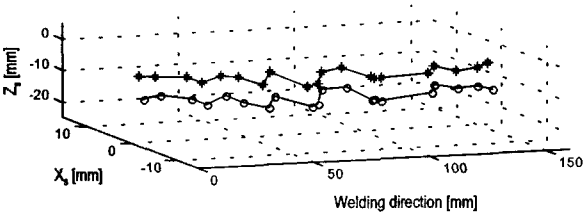

Fig. 16 Controlled x, z coordinate values against 5 degrees deviation

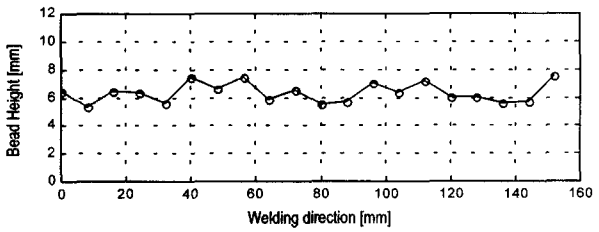

Fig. 17 Controlled bead heights against 5 degrees deviation

was performed successively. The application of LUT and erosion filtering made possible the elimination of the spatter noises intruded into the image. The experiment showed the warping of the work-pieces during welding could be dealt with fairly. Fig. 12 is the result with no control action against those disturbances mentioned and Fig. 13 is the one when the bead height is controlled and the weld seam tracked simultaneously against 5° offset angle. Fig. 14 shows the sensor coordinate z_S, measured on-line along the welding direction, where the cross point of the weld joint and the laser slit is indicated as O and the point that has maximum distance from the joint in the given angle range as *. It describes that, despite the changing joint point, the distance between the two symbols kept fairly constant. Fig. 15 shows that the coordinate x_S of the point on the bead surface is controlled to be positioned slightly to the right of the joint point in consideration of the gravitational force. The controlled bead distance against 5° offset angle is shown in Fig. 17. The pitching of the z_S coordinates in Fig. 14 is caused by the time delay due to the 30mm offset distance between the torch and the vision sensor.

Similar results were gained for the offset angles 3° and 4°. To summarize, though the oscillation of the z_S coordinate increased as the offset angle increased, the control and seam tracking was performed fairly well. Table 2 shows the average of the errors from the reference value, maximum error, and standard deviation for x_S and z_S against the offset angles 3°, 4° and 5° respectively. The errors for x_S coordinate that has comparatively larger control quantity increased

slightly as the angle increased, but the errors for z_S coordinate that has on the contrary smaller control quantity was kept relatively stable considering the fact that filler wire is 1.2mm in diameter.

Table 2 Control results against deviation angle 3°, 4° and 5°

Error / Offset angle	Average		Max error		STD	
	x_S	z_S	x_S	z_S	x_S	z_S
3 degrees	0.365	0.537	0.45	1.43	0.109	0.413
4 degrees	0.711	0.617	1.52	1.35	0.482	0.394
5 degrees	0.811	0.575	1.5	1.11	0.5	0.39

7. Conclusion

1. A vision system that can be applied both to seam tracking and weld quality monitoring was devised and it showed to be able to effectively eliminate varied noises in hardware and software related approaches.

2. A fuzzy controller which takes as input the position error and its derivative, and calculates as output the shift quantities for welding torch, was designed.

3. Real-time seam tracking through bead height and position control was performed against serious deformation due to the arc heat, gravitational force on the bead, and the varied offset angles.

References

1. P. Banerjee and B. A. Chin : Gradient technique for dynamic bead width control in robotic GTAW, *Trends in welding research*, Vol. 5, No. 1 (1995), pp. 937-941
2. P. L. Taylor : An integrated optical sensor for GMAW feedback control, *Trends in welding research*, Vol. 5, No. 1 (1995), pp. 1049-1053
3. R. J. Barnett, G. E. Cook, and A. M. Strauss : A vision-based weld quality evaluation system, *Trends in Welding Research, Proccedings of the 4th International Conference*, Vol. 4, (1995), pp. 689-694
4. D. H. Ballard and C. M. Brown : Computer vision, *Prentice-Hall, Inc.*, (1992), pp. 484-486
5. T. J. Ross : Fuzzy logic with engineering applications, *McGraw-Hill, Inc.*, (1995), pp. 469-508
6. A. Pugh : Robot sensors - vol. 1 - vision, International trends in manufacturing technology, *Springer -Verlag, Inc.*, (1986), pp. 159-204
7. J. E. Agapakis : Approaches for recognition and interpretation of work piece surface features using structured lighting, *The International Journal of Robotics Research*, Vol. 9, No. 5 (1990), pp. 3-16